Biophysical Reports, Volume *1*

Supplemental information

Fibrin prestress due to platelet aggregation and contraction increases clot stiffness

Suyog J. Pathare, Wilson Eng, Sang-Joon J. Lee, and Anand K. Ramasubramanian

S1. Materials and Methods

Acquisition of human blood

Blood was obtained from donor volunteers according to the protocol approved by the Institutional Review Board (F16134) at San José State University. The donors were 18 to 25 years of age, healthy, free of any known bleeding or cardiovascular disorders, nondiabetic, and not under any platelet-function altering medication. The blood was drawn in 3.2% buffered sodium citrate vacutainer tubes (BD Biosciences, San Jose, USA).

Preparation of blood clots

500 µL of blood was recalcified by the addition of sterile-filtered $CaCl_2$ (Millipore Sigma, St. Louis, MO, USA) at pH 7.4 to a final concentration of 20 mM, and restriction grade thrombin (Millipore Sigma, St. Louis, MO, USA) to a final concentration of 0.2 U/mL in wells of a 25 mm x 75 mm chamber slide (Nunc, Rochester, USA) and allowed to clot for 90 min at room temperature. For designated experiments, the following inhibitors were added to blood, and incubated for 30 min at room temperature with gentle rocking (Vari-Mix Platform Rocker, Thermo Fisher Scientific, Waltham, MA, USA) at approximately 2 Hz before recalcification: blebbistatin (Calbiochem, San Diego, CA, USA) at 300 µM; eptifibatide (Bio-Techne Corp., Minneapolis, MN) at 10 µM; or T101 (Zedira GmbH, Germany) at 10 µM.

Measurement of clot response to uniaxial strain

Design and fabrication of custom microtensometer device

The microtensometer consists of a motorized nanopositioner (MP-285, Sutter Instrument, Novato, CA, USA), a full-bridge thin cantilever load cell (113 g, LCL Series, OMEGA Engineering, Norwalk, CT, USA), and a signal conditioner DI-1000U (Loadstar Sensors, Fremont, CA). The nanopositioner has a 25 mm range resolution of 40 nm per step. Speeds are selectable from 20 µm/s to 2.9 mm/s. The DI-1000U has 24-bit resolution and up to 80 Hz sampling rate.

An aluminum clamp with a recessed crevice that allowed for two points of contact was found to provide consistent clamping. A magnet was press-fit inside the lower jaw of each clamp to create a clamping force with the upper jaw that had a steel screw attached. The magnetic clamping force was adjustable to prevent tearing while ensuring no slip, by adjusting the height of the screw and locking it in place with a counter-tightened nut.

Acquisition of force-displacement data

Clots were loaded in between two clamps with fine adjustment enabled by manually operated 3-axis micromanipulators (Cascade Microtech, Beaverton, OR, USA). Each clot began at 6 mm gauge length, and load cells were tared to zero before applying extension. The force recording from the data acquisition software (SensorVUE, Loadstar Sensors, Fremont, CA, USA) and actuation of the nanopositioner were started simultaneously and force measurements were recorded at 30 Hz. The clots were continuously strained to 3 mm at 100 µm/s which was 50% of the initial 6 mm gauge length. Each single experiment was completed within 3 minutes for any given clot including only 30 s for pulls, and replicate clots (typically three) in each set of runs were kept under plastic cover to prevent drying.

Estimation of cross-sectional area of the clot

Prior to applying strain, one digital microscope camera was set to capture top-view images of the clot to extract top cross-sectional dimensions, and a second digital camera was used to capture side-view images to extract thickness. The cameras captured images during the strain loading, each 8 s apart, to obtain true stress from force measurements. The cross-sectional area from the sequence of images were used to convert force measurements to true stress values. ImageJ software (NIH) was used to measure the three top-view images for the width *w* and two side images for thickness *t.* The area of the clot at 10 intervals along the length was calculated by measuring the width and thickness from the top and side view images taken.

S2. Analytical expression for force on prestressed fibrin fibers due to uniaxial tensile strain.

Each fiber element in **Fig. 5B** is assumed to have a linear relationship between axial stress σ and axial strain ε according to Hooke's law $\sigma = E\varepsilon$, where E is the elastic modulus. Letting $\hat{u}$ represent the axial displacement function along the element in the $\hat{e}$ direction, the strain in the element is $\varepsilon = d\hat{u}/d\hat{e}$, where the caret symbol (^) signifies a scalar direction that is always aligned with the longitudinal axis of the considered element. Equilibrium requires that the axial force $F = \sigma A$ be constant along the element, where A is the cross-sectional area of the element. Accordingly, the governing differential equation for the element is as shown in equation S2a.

$$\frac{d}{d\hat{e}}\left(EA\frac{d\hat{u}}{d\hat{e}} \right) = 0 \tag{S2a}$$

Assigning a linear displacement function for $\hat{u}$ and writing in terms of the nodal displacements $\hat{d}_{0x}$ and $\hat{d}_{1x}$ of the end nodes in local coordinates, the displacement function in matrix form is as shown in equation S2b.

$$\hat{u} = \begin{bmatrix} \left(1 - \dfrac{\hat{e}}{L}\right) & \dfrac{\hat{e}}{L} \end{bmatrix} \begin{Bmatrix} \hat{d}_{0x} \\ \hat{d}_{1x} \end{Bmatrix} \tag{S2b}$$

Equation S2c shows the corresponding stiffness equation for the element between node 0 and node 1, in terms of nodal forces $\hat{f}_{0x}$ and $\hat{f}_{1x}$.

$$\begin{Bmatrix} \hat{f}_{0x} \\ \hat{f}_{1x} \end{Bmatrix} = \frac{EA}{L} \begin{bmatrix} 1 & -1 \\ -1 & 1 \end{bmatrix} \begin{Bmatrix} \hat{d}_{0x} \\ \hat{d}_{1x} \end{Bmatrix} \tag{S2c}$$

Similarly, equation S2d shows the notation for a second element between node 1 and node 2.

$$\begin{Bmatrix} \hat{f}_{1x} \\ \hat{f}_{2x} \end{Bmatrix} = \frac{EA}{L} \begin{bmatrix} 1 & -1 \\ -1 & 1 \end{bmatrix} \begin{Bmatrix} \hat{d}_{1x} \\ \hat{d}_{2x} \end{Bmatrix} \tag{S2d}$$

By superposition and using distinct subscripts 1 and 2 for the respective values of area, modulus, and length of each fiber, the global stiffness equation for the two elements in series is shown in equation (S2e).

$$\begin{Bmatrix} F_{0x} \\ F_{1x} \\ F_{2x} \end{Bmatrix} = \begin{bmatrix} k_1 & -k_1 & 0 \\ -k_1 & k_1+k_2 & -k_2 \\ 0 & -k_2 & k_2 \end{bmatrix} \begin{Bmatrix} d_{0x} \\ d_{1x} \\ d_{2x} \end{Bmatrix} \tag{S2e}$$

By symmetry of placing node 0 at the origin of the quadrant, $d_{0x} = 0$. For tensometric loading, the end displacement d_{2x} is a prescribed value δ. There is no externally applied force at node 1, such that $F_{1x} = 0$. With these boundary conditions, the solution reduces to two equations and two unknown (S2f).

$$\begin{Bmatrix} 0 \\ F_{2x} \end{Bmatrix} = \begin{bmatrix} k_1+k_2 & -k_2 \\ -k_2 & k_2 \end{bmatrix} \begin{Bmatrix} d_{1x} \\ \delta \end{Bmatrix} \tag{S2f}$$

The solution to the scenario with only a prescribed external displacement is straightforward with $d_{1x} = k_2\delta/(k_1+k_2)$ and the axial force $F_{2x} = F$ as shown in equation (S2g).

$$F = \left(k_2 - \frac{k_2^2}{k_1+k_2} \right) \delta \tag{S2g}$$

The strain energy in each specific element i can be computed from stored elastic energy $\frac{1}{2}k_i u_i^2$ nodal displacements, where the axial displacement u_i is computed from the difference in nodal displacements (e.g., $u_1 = d_{1x} - d_{0x}$). The corresponding strain energy density for each element or for the overall system is computed by dividing by respective volume.

We make two important modifications to the basic two-element solution above for our pre-strained discrete fiber model. First, at node 1 (i.e., location of the focal adhesion) we add a contractile force $F = -\alpha EA$, for which the elastic modulus E and cross-sectional area A pertain to the platelet aggregate. Entering this force into the global stiffness equation and simplifying reduces the system to two equations (S2h).

$$\begin{Bmatrix} -\alpha EA \\ F_{2x} \end{Bmatrix} = \begin{bmatrix} k_1+k_2 & -k_2 \\ -k_2 & k_2 \end{bmatrix} \begin{Bmatrix} d_{1x} \\ \delta \end{Bmatrix} \tag{S2h}$$

The extent of aggregate compaction from an initial radius R_0 to a compacted radius R_c can be described either by the compaction strain α or alternatively in terms of compaction ratio $\zeta = R_0/R_c = 1/(1-\alpha)$. With compaction, the displacement at node 1 becomes $d_{1x} = (k_2\delta - \alpha EA)/(k_1 + k_2)$. Equation (S2i) shows the modified solution for axial force when prestrain is taken into account.

$$F = \left(k_2 - \frac{k_2^2}{k_1+k_2} \right) \delta + \frac{k_2 EA}{k_1+k_2} \alpha \tag{S2i}$$

Second, we account for multi-directional orientation of fibers using coordinate transformations for fibers that are oriented off-axis from the direction of externally applied strain. Coordinate transformation is achieved by using a rotation matrix to allow any

element oriented at an angle θ (measured counter clockwise from the global x-axis) to be mapped to global displacements d_x and d_y as shown in equation S2j.

$$\begin{Bmatrix} \hat{d}_x \\ \hat{d}_y \end{Bmatrix} = \begin{bmatrix} \cos(\theta) & \sin(\theta) \\ -\sin(\theta) & \cos(\theta) \end{bmatrix} \begin{Bmatrix} d_x \\ d_y \end{Bmatrix} \tag{S2j}$$

This prestress model formulation was verified using finite element analysis (FEA) by taking advantage of the "thermal force" analogy used to model thermal expansion and contraction. The FEA computational solutions matched analytical solutions exactly for the entire range of relative size, relative modulus, compaction ratio, and orientation angles.

S3. Supplementary Figures

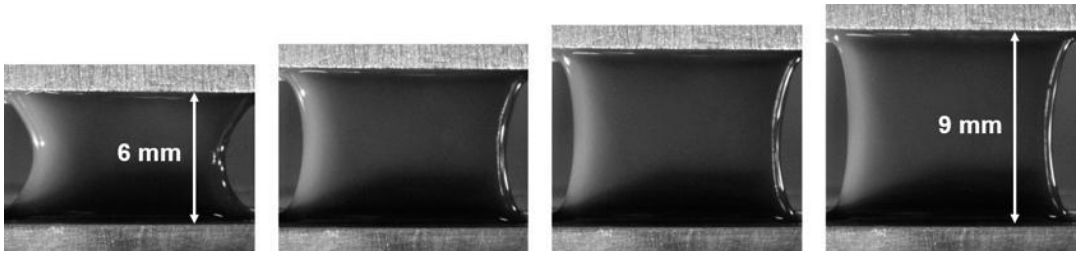

Figure S1. Real time images of clots as the clots are pulled by microtensometer to a maximum of 50% strain

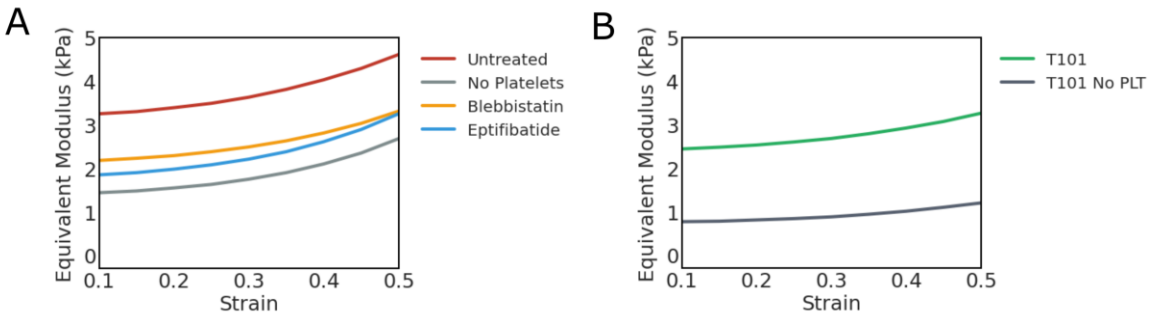

Figure S2. Equivalent modulus of the clots evaluated from the nonlinear exponential model at indicated strains.

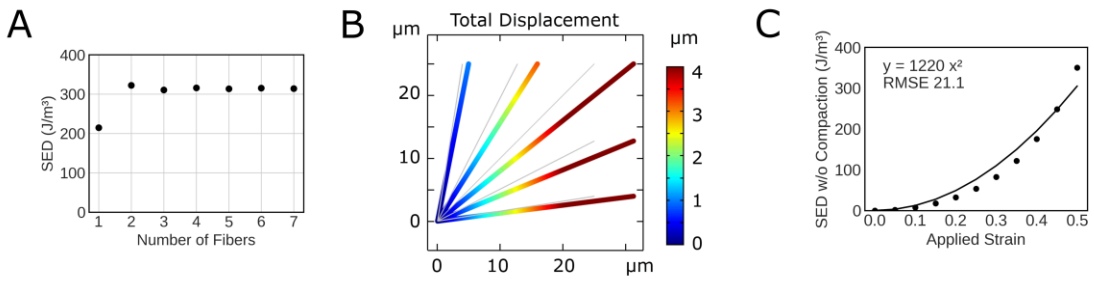

Figure S3. Characterization of discrete prestressed fiber model. (A) Convergence plot for strain energy density at 50% tensile strain and constant modulus (4.4 kPa), computed from a discrete fiber model consisting of different numbers of fibers; (B) Deformation of a prestressed fiber model of clot at 25% tensile strain without any platelet contraction (i.e., fibrin fibers only); (C) Strain energy density at 50% applied strain in the absence of any contractile strain shows approximately quadratic increase with externally applied strain, where RMSE = root mean square error.

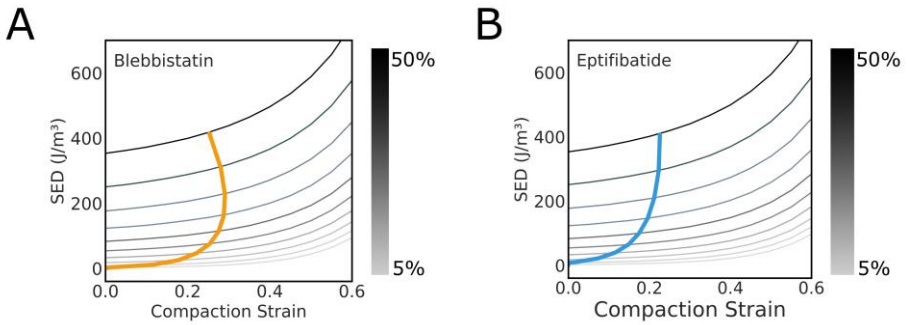

Figure S4. Mapping of experimental strain energy densities at applied strains from 5% to 50% onto predictions from discrete prestressed fiber model for blebbistatin (A) and eptifibatide (B) treatments.